Charge-transfer transition in two-dimensional $Cs[Co(3\text{-cyanopyridine})_2][W(CN)_8]\cdot H_2O$ as investigated by angle-resolved x-ray diffraction

J. E. Kim and Y. Ohishi
JASRI/SPring-8, Sayo-gun, Hyogo 679-5198, Japan

Y. Moritomo
Department of Physics, University of Tsukuba, Tsukuba 305-8571, Japan

K. Kato and M. Takata
RIKEN SPring-8 Center, 1-1-1 Kouto, Sayo-cho, Sayo-gun, Hyogo 679-5148, Japan

S. Ohkoshi
Department of Chemistry, University of Tokyo, Tokyo 113-0033, Japan

(Received 24 March 2007; revised manuscript received 25 May 2007; published 13 July 2007)

The structural properties were investigated for a two-dimensional cobalt octacyanotungsten, which shows temperature- and photoinduced *charge-transfer* (CT) transitions, by means of the synchrotron-radiation x-ray powder diffraction. We have found that the Co-W sheet nearly keeps the shape, but enlarges in size, at the CT transition from the Co^{3+}-W^{4+} configuration to the Co^{2+}-W^{5+} configuration. Based on the systematic investigation of the thermal treatment and photoirradiation effects on the structural properties, we will discuss the mechanism for the photoinduced CT transition.

DOI: 10.1103/PhysRevB.76.014106 PACS number(s): 64.70.Kb, 64.90.+b, 61.10.Nz

I. INTRODUCTION

The cyano-bridged metal complexes (CBMCs), -*M*-CN-*M'*-NC-*N*- (*M* and *M'* are metal ions), have been attracting renewed interest of materials scientists because they show novel photoinduced magnetization (demagnetization)[1–5] as well as the photoinduced structural change.[6,7] Especially, in the so-called Prussian Blue-like compound, $A^{I}M^{II}[M'^{III}(CN)_6]$ (A=Na, K, Rb, Cs, M=Mn, Co, Cr, M'=Fe, Cr)[1,2,8–12] the three-dimensional (3D) *M*-*M'* network is formed in the face-centered cubic ($Fm\bar{3}m$; Z=4) structure. In addition, the dimensionality of the *M*-*M'* network can be controlled by the ligand substitution: for example, $Mn_9[W(CN)_8]\cdot 24C_2H_5OH\cdot 12C_2H_5OH$ has a zero-dimensional (0D) structure,[13] while $Cs[Co(3\text{-CNpy})_2]W(CN)_8\cdot H_2O$ (CNpy=cyanopyridine) has a two-dimensional (2D) Co-W network.[5] A characteristic feature of the CBMC is the thermally and photoinduced *charge-transfer* (CT) transition, i.e., cooperative charge transfer between the neighboring metal ions, *M* and *M'*. The CT transition usually accompanies a significant structural change, which modifies the spin state of *M* and *M'*, the exchange interaction between *M* and *M'* (magnetism), and the charge-transfer excitation energy between *M* and *M'* (color). In this sense, investigation of the structural properties, especially the configuration of the *M*-*M'* network, is indispensable for deeper comprehension of the CT transition as well as the physical properties in both the phases.

$Cs[Co(3\text{-CNpy})_2][W(CN)_8]\cdot H_2O$ consists of the cyano-bridged Co-W sheets stacking along the *b* direction in the triclinic ($P\bar{1}$, Z=2) setting.[5] Among the eight CN moieties of the octacyanotungsten ($[W(CN)_8]$), four are linked to the neighboring Co atoms to form a zigzag sheet, as shown in Fig. 1. This compound shows the thermally induced CT transition at T_{CT}=216 K from the Co^{3+} (S=0)-W^{4+} (S=0) configuration to the Co^{2+} ($S=\frac{3}{2}$)-W^{5+} ($S=\frac{1}{2}$) configuration. At the transition, the sample color changes from dark green to transparent red. The same CT transition is further induced by photoirradiation of a visible light (600–750 nm, 12.5 mW cm^{-2}) at 5 K, which causes the photoinduced magnetization.[5] Yokoyama *et al.*[14] investigated the effects of thermal treatment, photoirradiation, and x-ray irradiation on the structural properties of $Cs[Co(3\text{-CNpy})_2]\times[W(CN)_8]\cdot H_2O$ by means of the x-ray absorption fine structure (XAFS) spectroscopy. They found that the Co–N bond distance elongates by ≈0.17 Å at the CT transition.

In this paper, we have investigated effects of the thermal quenching and the photoirradiation on the structural properties of $Cs[Co(3\text{-CNpy})_2]W(CN)_8\cdot H_2O$ by means of the synchrotron-radiation (SR) x-ray powder diffraction. We found that the Co-W bond distance elongates by ≈0.21 Å at the CT transition. We further found that the W atom shows a characteristic out-of-sheet movement (see arrows in Fig. 1) at the transition, which is considered to be an origin for the

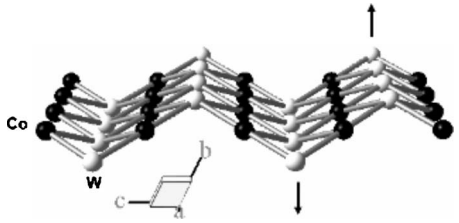

FIG. 1. Cyano-bridged Co-W layer of $Cs[Co(3\text{-CNpy})_2]W(CN)_8\cdot H_2O$. White and black circles represent W and Co, respectively. Arrows indicate the out-of-plane movement of the W atoms.

 ©2007 The American Physical Society

slow relaxation time τ of the matastable state. Based on these structural features, we will propose a possible scenario for the photoinduced CT transition.

II. EXPERIMENT

$Cs[Co(3\text{-}CNpy)_2][W(CN)_8]\cdot H_2O$ was prepared by adding an aqueous solution of $Cs_3[W(CN)_8]$ (0.1*M*) to a mixed aqueous solution of $CoCl_2$ (0.1*M*) and 3-CNpy (0.2*M*) at room temperature. After 24 h, the precipitated red powders were gathered and washed with water. Details of the sample characterization were described in Ref. 5.

The SR x-ray powder diffraction experiments were carried out with a large Debye-Scherrer camera (r =286.5 mm ϕ) installed at BL02B2 beamline of the SPring-8.[15] The typical exposure time was 5 min. In order to get a homogeneous intensity distribution in the Debye-Scherrer powder ring, the as-grown powders were carefully crashed into fine powders. The fine powders were sealed in a quartz capillary, 100 μm in diameter. The homogeneity of the ring is a necessary condition for a reliable Rietveld analysis. The wavelength of the incident x-ray was 0.828 66 Å, which was calibrated with the use of standard CeO_2 powders obtained from NIST. The collimator size was 0.5×3 mm^2.

In the measurements of the "photoirradiated" diffraction patterns,[6,7] the sample powders were mixed with glass powders to perform a homogeneous irradiation at 100 K. The excitation light source was a continuous-wave laser (532 nm, 10 mW/mm^2), and excitation period was for 30 min. In the measurements of the "thermally quenched" diffraction patterns, the sample at 300 K was blown by the cold nitrogen gas whose temperature was controlled at 100 K. In order to complete the phase transition into the low-temperature (LT) phase, the sample temperature was slowly (≈1 K/min) decreased near the melting point (≈130 K, *vide infra*) of the matastable state.

In order to reveal the kinetic aspect of the diffraction pattern, a much shorter exposure time was adopted. In Sec. III C, we investigated the relaxation behavior of the matastable state. In this experiment, the exposure time was set to 30 s, and the starting time for the respective measurement was monitored. In Sec. III D, we investigated the x-ray irradiation effect. This experiment was performed with a flat imaging plate installed at the BL10XU beamline of the SPring-8. The fine powders were sandwiched between tapes. The wavelength of the incident x ray was 0.623 05 Å, which was calibrated with the use of standard CeO_2 powders obtained from NIST. The x-ray beam size was 0.1 mm ϕ. In this experiment, x-ray beam was used as both the excitation source and the probe source. We investigated the diffraction pattern every 120 s.

III. RESULTS

A. Rietveld analysis

Figure 2 shows the magnified x-ray diffraction patterns of $Cs[Co(3\text{-}CNpy)_2][W(CN)_8]\cdot H_2O$ at 100 K. The top pattern is for the LT phase obtained after careful thermal treatment, as described in Sec. II. The second (third) pattern was obtained at 100 K after photoirradiation (thermal quenching). These patterns are significantly different from the LT pattern (top) but rather resemble the high-temperature (HT) pattern (bottom). This suggests that the photoirradiation as well as the thermal quenching produces a HT-like structure.

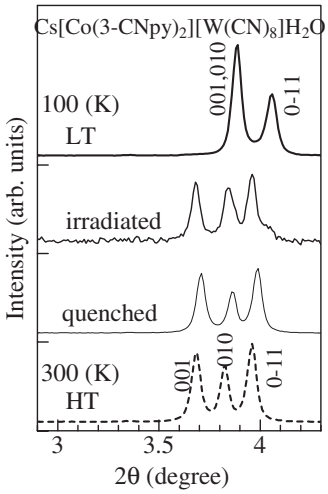

FIG. 2. Magnified x-ray diffraction patterns of $Cs[Co(3\text{-}CNpy)_2]W(CN)_8\cdot H_2O$ at 100 K (upper three patterns). Wavelength of the x-ray was 0.828 66 Å. LT and HT represent the low-temperature phase and high-temperature phase, respectively. The "irradiated" pattern was obtained after photoirradiation by a continuous-wave laser (532 nm, 10 mW/mm^2) for 30 min. The "quenched" pattern is obtained after thermal quenching at 100 K. The lowest pattern is for the HT phase at 300 K. The exposure time was 5 min (60 min). for the "irradiated" pattern and the "quenched" pattern (HT phase and LT phase).

We have analyzed these diffraction patterns shown with the Rietveld procedure with the triclinic ($P\bar{1}$,[5] Z=2) space group. As an example, we show in Fig. 3 the fitting result for the LT phase at 100 K. The reliable factors, R_{wp} and R_I, are 4.57% and 4.85%, respectively. Thus, obtained cell param-

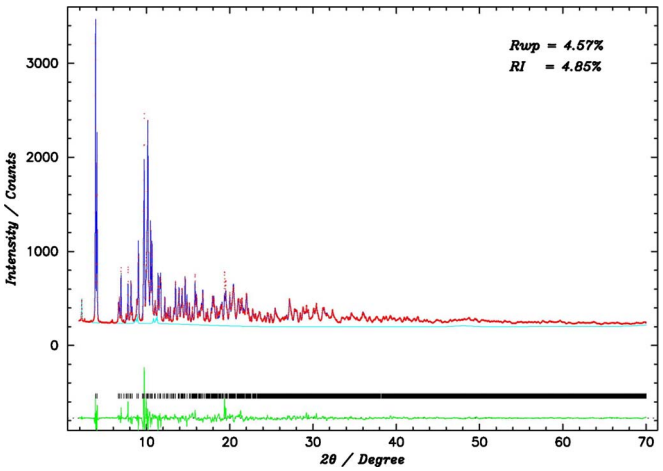

FIG. 3. (Color online) Rietveld fitting of the x-ray diffraction pattern of $Cs[Co(3\text{-}CNpy)_2]W(CN)_8\cdot H_2O$ at 100 K. Solid curve and dots are the calculated result and the experimental data, respectively. The bars present the calculated reflection positions. The bottom curve is the difference between the calculation and experiment.

TABLE I. The cell parameters of $Cs[Co(3\text{-}CNpy)_2]\times[W(CN)_8]\cdot H_2O$ in the triclinic ($P\bar{1}$, $Z=2$) setting for the low-temperature (LT) phase at 100 K, the "irradiated" sample at 100 K, the "quenched" sample at 100 K, and the high-temperature (HT) phase at 300 K. v represents the cell volume. The reliable factors are defined as $R_{wp}\equiv\left[\frac{\Sigma_i w_i(y_i-y_{i,calc})^2}{\Sigma_i w_i y_i^2}\right]^{1/2}$ and $R_I\equiv\frac{\Sigma_K|I_{K,calc}-I_K|}{\Sigma_K I_{K,calc}}$.

	LT (100 K)	Irradiated	Quenched	HT (300 K)
a (Å)	7.1245(2)	7.3067(7)	7.2911(3)	7.3157(2)
b (Å)	13.8479(4)	13.844(1)	13.8200(5)	13.9564(4)
c (Å)	13.6980(4)	14.336(1)	14.3066(5)	14.3791(4)
α (deg)	116.854(2)	116.379(8)	116.371(3)	116.223(2)
β (deg)	90.008(2)	89.997(6)	90.008(3)	90.010(2)
γ (deg)	97.702(3)	96.598(8)	96.596(3)	97.068(3)
v (Å^3)	1192.00(7)	1288.4(2)	1290.89(9)	1304.48(15)
R_{wp}	4.57	2.71	5.67	4.64
R_I	4.85	13.86	5.59	5.12

eters are listed in Table I, together with the reliable factors. Taking account of the thermal contraction of the cell parameters, we concluded that the metastable structures of the "irradiated" sample and the "quenched" sample are essentially the same as that of the HT phase.

B. Thermal stability of the metastable state

In order to investigate the thermal stability of the metastable state, we measured the temperature dependence of the x-ray diffraction patterns of the irradiated sample (thick curves) and quenched sample (thin curves) in the warming run (see Fig. 2). In this measurement, the sample temperature was stepwise increased every 20 K with the holding time of 10 min (including the exposure time of 5 min). Both the powder patterns change into that of the LT phase as temperature increases, indicating the melting of the HT structure into the LT structure. We estimated the volume fraction n_{HT} of the HT phase by a two-phase Rietveld analysis of the powder patterns and plotted them in Fig. 5(a). In both the phases, the magnitude of n_{HT} steeply decreases at ~130 K. This steep reduction of n_{HT} is ascribed to the fast relaxation of the metastable HT structure.

The slight difference observed in the melting behavior [see Figs. 4 and 5(a)] can be ascribed to the different domain structure between the irradiated sample and the quenched sample. Hanawa *et al.*[6] investigated the photoirradiation effect on a Prussian Blue-like compound, $Na_{0.42}Co[Fe(CN)_6]_{0.78}\cdot 4.64H_2O$, and compared the metastable state of the irradiated sample and the quenched sample. They found that the domain size of the metastable state is much larger in the irradiated sample. Even though the domain size is large (~1 μm) in the present Co-W cyanide system, its difference can cause the different melting behavior, as observed.

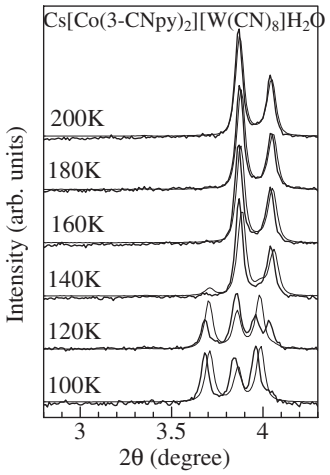

FIG. 4. Temperature dependence of the x-ray diffraction patterns of the "irradiated" sample (thick curves) and "quenched" sample (thin curves) in the warming run. Wavelength of the x ray was 0.828 66 Å. The sample temperature was stepwise increased every 20 K with the holding time of 10 min (including the exposure time of 5 min).

Here, let us comment on the heating effect inevitably induced by photoirradiation. Figure 5(b) shows the temperature variation of n_{HT} in the warming run. In this measurement, the sample temperature was stepwise increased every 20 K with the holding time of 10 min (including the exposure time of 5 min). Without photoirradiation (closed circles), the magnitude of n_{HT} steeply increases at T_{CT} ~190 K. The apparent increase (ΔT_{CT}~30 K) of T_{CT} under photoirradiation (open circles) should be ascribed to the heating. The temperature rise, however, is insufficient to cause the CT trasition at 100 K. This clearly indicates that the photoinduced CT transition cannot be ascribed to the conventional heating effect.

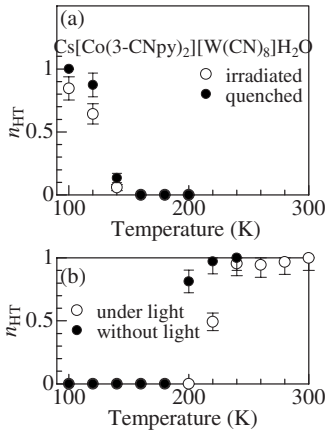

FIG. 5. (a) Volume fraction n_{HT} of the HT phase in the "irradiated" sample (open circles) and "quenched" sample (closed circles) in the warming run. (b) n_{HT} in the warming run under photoirradiation (open circles) and without photoirradiation (closed circles). The magnitude of n_{HT} was determined by Rietveld refinement with a two-phase model. The sample temperature was stepwise increased every 20 K with the holding time of 10 min (including the exposure time of 5 min).

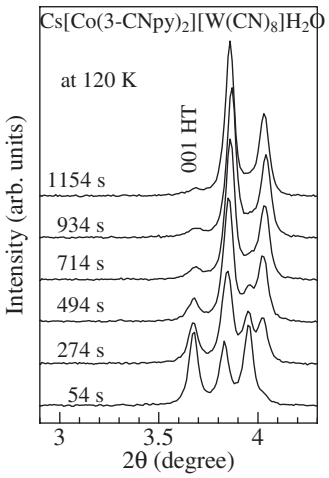

FIG. 6. Temporal behavior of the x-ray diffraction patterns of the "quenched" sample measured at 120 K. Wavelength of the x ray was 0.828 66 Å. The diffraction patterns (exposure time was 30 s) were obtained every 110 s. The time is the starting time of the respective measurement.

C. Melting process of the metastable state

In order to investigate the melting process, we measured the temporal behavior of the x-ray diffraction patterns of the quenched sample at 120, 125, and 130 K. In Fig. 6, we show the temporal behavior of the diffraction pattern measured at 120 K. In this experiment, the diffraction patterns were obtained every 110 s (including the exposure time of 30 s). The diffraction patterns change into that of the LT phase with time, indicating the melting of the HT structure into the LT structure.

We roughly estimated n_{HT} by the intensity from the intensity of the (001) reflection of the HT phase[16] and plotted them in Fig. 7(a). We have estimated the relaxation time τ at each temperature by the least-squares fitting with the exponential function: $\tau \approx 170$ s at 130 K, $\tau \approx 284$ s at 125 K, and $\tau \approx 341$ s at 120 K. Here, let us argue the effect of the required time (20–40 s) to increase the sample temperature. This required time effectively shifts the starting point of the experiment because the sample temperature is lower than the setting temperature in the early stage. We believe that this effect is not serious in determination of τ because the shift only changes the prefactor of the exponential function.

As shown in Fig. 7(b), these τ values nearly obey the Arrhenius law: $\tau = 0.045 \exp\left(\frac{1092}{T(\mathrm{K})}\right)$. We emphasize that the obtained activation energy Δ (=0.094 eV) is fairly small, as compared with that of the other the CBMCs. For example, Δ is reported to be ≈ 0.23 eV (Ref. 17) in $Na_{0.42}Co[Fe(CN)_6]_{0.72} \cdot 4.6H_2O$ with a 3D cyano-bridged metal network. We ascribed the small Δ to the characteristic zigzag Co-W sheet structure (Fig. 1). Actually, we found that the heavy W atom (or the $[W(CN)_8]$ unit) shows an out-of-sheet movement at the CT transition (*vide infra*). Such a motion causes the small potential barrier between the two saddle points because the contraction of the Co-W bond distance accompanies the bending of the W-Co-W bond angle. In addition, the slow motion of the heavy W atom is consistent with the rather large prefactor (=0.045 s) of the Arrhenius law.

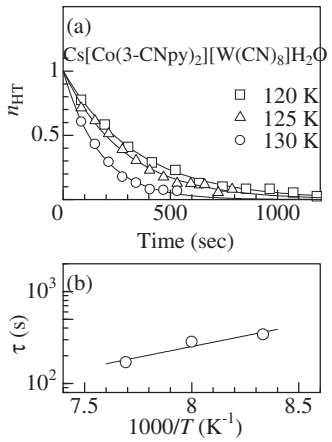

FIG. 7. (a) Volume fraction n_{HT} of the HT phase in the "quenched" sample against time. The melting procedure was measured at 120 K (open squares), at 125 K (open triangles), and at 130 K (open circles). The magnitude of n_{HT} was estimated by the intensity of the (001) reflection of the HT phase. The solid curves are the results of the least-square fitting with an exponential function: $n_{\mathrm{HT}} = \exp\left(-\frac{t}{\tau}\right)$. (b) Arrhenius plot of the relaxation time τ: $\tau = 0.045 \exp\left(\frac{1092}{T(K)}\right)$.

D. X-ray irradiation effect

Here, let us briefly comment on the x-ray irradiation effect on the lattice structure. Yokoyama *et al.*[14] reported an x-ray-induced change of the XAFS spectra around the Co *K* edge at 30 K. They concluded that the Co^{3+} density gradually decreases under irradiation of x ray, whose energy and photon flux were ≈ 7.7 keV and $\sim 10^{11}$ photon/s mm^2, respectively. In our experiment, the x-ray energy and photon flux were 15.0 keV and $\sim 10^{11}$ photon/s mm^2, respectively. We, however, observed no detectable change in the diffraction patterns measured at 100 and 300 K even after 1 h x-ray irradiation. The different x-ray irradiation effect may be ascribed to the different x-ray energy because the x-ray energy of the former experiment resonates to the Co *K* edge.

Even in the off-resonant condition, a significant x-ray irradiation effect was observed if we increase the photon flux up to $\sim 10^{14}$ photon/s mm^2. Figure 8 shows the x-ray irradiation time dependence of the diffraction patterns of $Cs[Co(3\text{-}CNpy)_2][W(CN)_8] \cdot H_2O$ at 300 K, measured at the BL10XU beamline of SPring-8. The x-ray energy was 19.9 keV. The x-ray irradiation seems to shift the (001) and (010) reflections to the low-2θ side and to shift the (0−11) reflection to the high-2θ side. This suggests the variation of the cell parameters, i.e., a, b, c, α, β, and γ, with time. So, we tried to refine the cell parameters by the Rietveld fitting with the triclinic ($P\bar{1}$, $Z=2$) space group. The deformed profile of the diffraction pattern at higher-2θ region (not shown), however, prevents the reliable Rietveld fitting even at $t = 120$ s data.

IV. DISCUSSION

Now, let us investigate the detailed configuration of the Co-W sheet as well as the structural variation at the CT

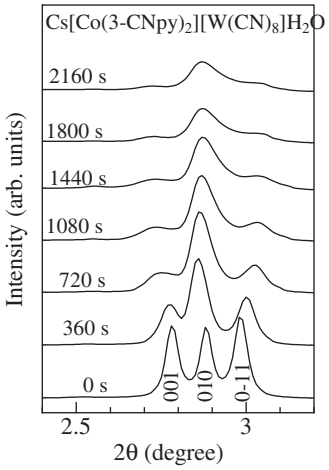

FIG. 8. Magnified x-ray diffraction patterns of $Cs[Co(3\text{-}CNpy)_2]W(CN)_8 \cdot H_2O$ at 300 K against the x-ray irradiation time. Wavelength of the irradiated x ray was 0.623 05 Å. The photon flux was $\sim 10^{14}$ photon/s mm^2. The exposure time was 120 s for each measuremet. The time is the starting time of the respective measurement.

transition. In Table II, we listed the bond distances, the bond angles, and the atomic coordinates of the Co-W sheet in the LS phase and the HT phase. One of the most significant features is the elongation of the Co-W bond distance $d_{\text{Co-W}}$ by ≈ 0.21 Å at the CT transition.[18] In crystallographical point of view, this elongation shows up as the increase of the cell parameters. Especially, a (c) increases by 3% (5%) at the phase transition (see Table I). In addition, we note that the y coordinate of the W atom increases by 5% at the CT transition. In other words, the W atom gets away from the Co plane to elongate the Co-W bond distance. Reflecting these structural features, i.e., (1) the increase of a and c and (2) the out-of-sheet movement of the W atom (see arrows in Fig. 1), the Co-W sheet nearly keeps the shape, but enlarges in size, at the CT transition.

Finally, let us discuss the mechanism for the photoinduced CT transition based on the above-mentioned structural features of the Co-W sheet. The first process of the photoexcitation is the charge-transfer excitation from the W^{4+} site to the Co^{3+} site, which creates the so-called Frank-Condon state. The Co-W bond distance would locally increase with this electronic configuration because the ionic radius $r_{\text{HSCo}^{2+}}$ [=0.745 Å (Ref. 19)] of the HS Co^{2+} ion is much larger than $r_{\text{LSCo}^{3+}}$ [=0.545 Å (Ref. 19)] of the LS Co^{3+} ion. Such a bond elongation is considered to be achieved by the pendular movement of the W atom because the motion keeps the other two Co-W bond distances. Resultant local lattice relaxation stabilizes the charge-transferred state. Then, these charge-transferred states gradually accumulate by the subsequent photoexcitations and eventually induce a macroscopic structural phase transition into the HT phase when the density of the charge-transferred states exceeds a critical value.

TABLE II. Bond distances and bond angles within the Co–W sheet of $Cs[Co(3\text{-}CNpy)_2][W(CN)_8] \cdot H_2O$ in the LT phase and the HT phase. The atomic positions, Co1 $\left(-\frac{1}{2},0,\frac{1}{2}\right)$, Co2 $\left(-\frac{1}{2},0,0\right)$, and W (x,y,z), are also shown.

	LT (100 K)	HT (300 K)
$d_{\text{Co1–W}}$ (Å)	5.136(2)	5.334(2)
$d_{\text{Co1–W}}$ (Å)	5.160(2)	5.372(2)
$d_{\text{Co2–W}}$ (Å)	5.151(2)	5.354(3)
$d_{\text{Co2–W}}$ (Å)	5.175(2)	5.390(3)
average (Å)	5.155(2)	5.362(3)
$\theta_{\text{Co1–W–Co2}}$ (degree)	146.85(6)	146.01(6)
x	0.0338(3)	0.0334(4)
y	0.1204(1)	0.1264(2)
z	0.3058(2)	0.3052(2)

V. SUMMARY

In summary, we have investigated the structural properties of the CT transition of a CBMC, $Cs[Co(3\text{-}CNpy)_2]W(CN)_8 \cdot H_2O$, with 2D cyano-bridged Co-W sheet. We have found that the Co-W sheet nearly keeps the shape, but enlarges in size, at the CT transition from the Co^{3+} ($S=0$)-W^{4+} ($S=0$) configuration to the Co^{2+} $\left(S=\frac{3}{2}\right)$-$W^{5+}$ $\left(S=\frac{1}{2}\right)$ configuration. We propose that the out-of-sheet movement of the heavy W atom plays an essential role not only in the thermal quenching of the HT phase but also the photoinduced CT transition at low temperatures.

ACKNOWLEDGMENTS

This work was supported by a Grant-in-Aid for Scientific Research from the Ministry of Education, Culture, Sports, Science and Technology, Japan and from the CREST project "X-ray pinpoint structural measurement project" from Japan Science Technology Agency. The synchrotron-radiation x-ray powder experiments were performed at the SPring-8 BL02B2 and BL10XU with the approval of the Japan Synchrotron Radiation Research Institute (JASRI).

[1] O. Sato, T. Iyoda, A. Fujishima, and K. Hashimoto, Science **272**, 704 (1996).

[2] O. Sato, Y. Einaga, T. Iyoda, A. Fujishima, and K. Hashimoto, J. Electrochem. Soc. **144**, L11 (1997).

[3] S. Ohkoshi, H. Tokoro, M. Utsunomiya, M. Mizuno, M. Abe, and K. Hashimoto, J. Phys. Chem. **106**, 2423 (2002).

[4] H. Tokoro, S. Ohkoshi, and K. Hashimoto, Appl. Phys. Lett. **82**, 1245 (2003).

[5] Y. Arimoto, S. Ohkoshi, Z. J. Zhong, H. Sekine, Y. Mizobe, and K. Hashimoto, J. Am. Chem. Soc. **125**, 9240 (2003).
[6] M. Hanawa, Y. Moritomo, A. Kuriki, J. Tateishi, K. Kato, M. Takata, and M. Sakata, J. Phys. Soc. Jpn. **72**, 987 (2003).
[7] Y. Moritomo, M. Hanawa, Y. Ohishi, K. Kato, M. Takata, A. Kuriki, E. Nishibori, M. Sakata, S. Ohkoshi, H. Tokoro, and K. Hashimoto, Phys. Rev. B **68**, 144106 (2003).
[8] T. Mallah, S. Thiebaut, M. Verdaguer, and P. Veillet, Science **262**, 1554 (1993).
[9] S. Ferlay, T. Mallah, R. Ouahes, P. Veillet, and M. Verdaguer, Nature (London) **378**, 701 (1995).
[10] S. Ohkoshi, M. Mizuno, G. J. Hung, and K. Hashimoto, J. Phys. Chem. B **104**, 9365 (2000).
[11] S. M. Holmes and G. S. Girolami, J. Am. Chem. Soc. **121**, 5593 (1999).
[12] O. Hatlevik, W. E. Bushmann, J. Zhang, J. L. Manson, and J. S. Miller, Adv. Mater. (Weinheim, Ger.) **11**, 914 (1999).
[13] Z. J. Zhong, H. Sekine, Y. Mizobe, M. Hidai, A. Fujishima, S. Ohkoshi, and K. Hashimoto, J. Am. Chem. Soc. **122**, 2952 (2000).
[14] T. Yokoyama, K. Okamoto, T. Ohta, S. I. Ohkoshi, and K. Hashimoto, Phys. Rev. B **65**, 064438 (2002).
[15] E. Nishibori, M. Takata, K. Kato, M. Sakata, Y. Kubota, S. Aoyagi, Y. Kuroiwa, M. Yamakawa, and N. Ikeda, Nucl. Instrum. Methods Phys. Res. A **467-468**, 1045 (2001).
[16] The absolute magnitudes of n_{HT} were determined so that the extrapolation of n_{HT} becomes 1 at $t=0$.
[17] T. Yamauchi, A. Nakamura, Y. Moritomo, T. Hozumi, K. Hashimoto, and S. Ohkoshi, Phys. Rev. B **72**, 214425 (2005).
[18] Yokoyama *et al.*[14] reported that the elongation Δd_{Co-N} of the Co–N bond distance is ≈ 0.17 Å. Judging from the slight reduction of the ionic radius of the W ion ($\Delta r_W = -0.04$ Å), our data ($\Delta d_{Co-W} = 0.21$ Å) are slightly larger than the value estimated by Yokoyama *et al.*.
[19] R. D. Shannon, Acta Crystallogr., Sect. A: Cryst. Phys., Diffr., Theor. Gen. Crystallogr. **32**, 1751 (1976).